Journal of Neuroscience Methods 212 (2013) 114–123

Contents lists available at SciVerse ScienceDirect

Journal of Neuroscience Methods

journal homepage: www.elsevier.com/locate/jneumeth

Basic Neuroscience

An MEG compatible system for measuring skin conductance responses

Charalampos Styliadis[a,1], Christos Papadelis[b,*,1], Evdokimos Konstantinidis[a], Andreas A. Ioannides[c], Panagiotis Bamidis[a]

[a] Laboratory of Medical Informatics, School of Medicine, Aristotle University of Thessaloniki, P.O. Box 323, 54124 Thessaloniki, Greece
[b] Department of Neurology, Children's Hospital Boston, Harvard Medical School, 9 Hope Av., 02453 Waltham, USA
[c] Laboratory for Human Brain Dynamics, AAI Scientific Cultural Services Ltd., Office 501, Galaxias Building Block A, 33 Arch. Makarios III Avenue, 1065 Nicosia, Cyprus

HIGHLIGHTS

- Magnetoencephalography compatible low-cost system for monitoring skin conductance responses in the magnetically shielded room.
- The system allows high quality simultaneous recordings of SCRs and MEG signals.
- Its implementation calls for limited knowledge in electronics due to its simplicity.

GRAPHICAL ABSTRACT

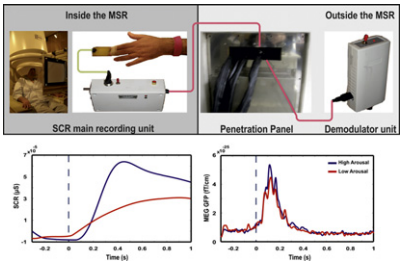

ARTICLE INFO

Article history:
Received 15 May 2012
Received in revised form
18 September 2012
Accepted 22 September 2012

Keywords:
Skin conductance response (SCR) system
Magnetoencephalography (MEG)
Magnetically shielded room (MSR)

ABSTRACT

We present the design of a low-cost system for recording galvanic skin conductance responses (SCRs) from humans in a magnetically shielded room (MSR) simultaneously to magnetoencephalography (MEG). Such a system was so far not available to the MEG community. Its availability is of utmost importance for neuroscience, since it will allow the concurrent assessment of the autonomic and central nervous system activity. The overall system design optimizes high signal to noise ratio (SNR) of SCRs and achieves minimal distortion of the MEG signal. Its development was based on a fiber-optic transformer, with voltage to optical transduction inside the MSR and demodulation outside the MSR. The system was calibrated and tested inside the MEG environment by using a 151-channel CTF whole head system (VSM MedTech Ltd.). MEG measurements were recorded simultaneously to SCRs from five healthy participants to test whether the developed system does not generate artifacts in the MEG data. Two measurements were performed for each participant; one without the system in the MSR, and one with the system in the MSR, connected to the participant and in operation. The data were analyzed using the time and frequency domains in separate statistical analysis. No significant differences were observed between the two sessions for any statistic index. Our results show that the system allows high quality simultaneous recordings of SCRs and MEG signals in the MSR, and can therefore be used as routine addendum to neuroscience experiments.

Abbreviations: SCRs, skin conductance responses; MSR, magnetically shielded room; SNS, sympathetic nervous system; ERPs, event-related potentials; MR, magnetic resonance; RF, radio-frequency; PSD, Power Spectral Density; SK, spectral kurtosis; VCO, voltage-controlled oscillator; EOG, Electrooculographic; ECG, electrocardiographic; MTM, Multitaper Method; GFP, global field power; IAPS, International Affective Picture System; PHA, pleasant and high arousing; PLA, pleasant and low arousing; UHA, unpleasant and high arousing; ULA, unpleasant and low arousing; SAM, Synthetic Aperture Magnetometry; IPF, inferior parietal lobule; TP, temporal pole; MNI, Montreal Neurological Institute.

* Corresponding author at: Baby MEG/EEG Facility, Department of Neurology, Children's Hospital Boston, Harvard Medical School, 9 Hope Av., 02453 Waltham, USA. Tel.: +1 781 216 1128; fax: +1 781 216 1172.
E-mail address: christos.papadelis@childrens.harvard.edu (C. Papadelis).
[1] Shared first authorship.

0165-0270/$ – see front matter © 2012 Elsevier B.V. All rights reserved.
http://dx.doi.org/10.1016/j.jneumeth.2012.09.026

1. Introduction

In response to different kinds of stimuli, part of the human sympathetic nervous system (SNS) is activated filling up the palmar and plantar sweat glands and as a consequence resulting in alterations of the human skin electrical properties (Boucsein, 1992). These skin conductance changes, termed skin conductance responses (SCRs), can easily be recorded via a pair of electrodes usually placed on the hand digits of a human participant. The temporal features of the SCR are well characterized with an onset latency of 1.5 s and a rise in skin conductivity thereafter that is proportional to the degree of synchronization of sweat gland secretions (Lim et al., 2003). SCRs are frequently used in neuroscience research as an indirect measure of human's emotional arousal (Bernat et al., 2006; Ohira et al., 2006; Lithari et al., 2010), level of attention (Critchley et al., 2000), or learning (MacIntosh et al., 2007).

Neuroscience studies of concurrent central and autonomic activity are considered useful in elucidating the relationship between central and autonomic responses. Traditionally, SCRs have been studied in conjunction with event-related potentials (ERPs) recorded by electroencephalography (EEG) that provide excellent temporal but limited spatial resolution.

Over the years, magnetoencephalography (MEG) has proven to be a reliable neuroimaging tool in studying electro-magnetic activity in the cortex (Hamalainen et al., 1993) offering – under favorable circumstances – a good spatial resolution of few millimeters (Yamamoto et al., 1988; Moradi et al., 2003; Papadelis et al., 2009, 2011) in addition to its sub-millisecond temporal resolution. MEG measures the weak (10 fT–1 pT) magnetic fields produced by neuronal currents in the human brain. Since the brain neuromagnetic signals are extremely weak compared with ambient magnetic-field variations, MEG requires the measurements to be performed within specially designed magnetically shielded rooms (MSRs). This technical requirement makes problematic the use of electrical devices placed in the MSR and thus the simultaneous recording of MEG signal and SCRs. Electronic devices need to be shielded, since otherwise will generate severe technical artifacts distorting the MEG signal.

Since now, there is no well-established methodological framework allowing the simultaneous acquisition of SCR with MEG. The literature reporting such kind of measurements is limited to only a single study (Seth et al., 2006), in which technical issues are not addressed in detail. This article addresses the technical aspects of monitoring SCR on human participants in the MSR during MEG measurements. The work presented here realizes in part the ideas and directions set in collaboration between the Laboratory of Medical Informatics, School of Medicine, Aristotle University of Thessaloniki and the Laboratory for Human Brain Dynamics at the Brain Science Institute, RIKEN (1998–2009) and its continuation at the AAI Scientific Cultural Services Ltd. in Cyprus. The principal goal of this collaboration was the design and implementation of a cheap and accurate measure of SCR that can be used both in studies with expensive state of the art MEG and fMRI equipment and in studies with simpler instrumentation, notably few-channel EEG. The system is therefore ideal for studies of affect and emotion, serves the growing battery of neurophysiological measurements required and the human–computer interaction that may accompany it (Bamidis et al., 2004). It is also ideal for measurements with children and patients under stressful tests where subtle features of the EEG response (Ioannides and Sargsyan, 2012) must be studied together with indices of arousal and anxiety levels.

To achieve these goals, we developed a low cost MEG-compatible system able to record SCRs with high signal to noise ratio (SNR) while not adversely distorting the MEG recordings. The design of our system was partially based on a device proposed by Shastri et al. (2001) for monitoring SCRs in a clinical magnetic resonance (MR) scanner during functional imaging. This functional magnetic resonance imaging (fMRI)-compatible device was initially built and tested in a MEG experimental setup. It was found to be non-MEG compatible, since it generated severe technical artifacts in the recorded MEG signal. To overcome this problem, a second MEG-compatible unit was designed and built employing an optical isolation serving to the signal transduction between the recording unit placed inside and the transforming unit placed outside the MSR. The special feature of our system is the optical isolation between the two units one placed inside and the other outside the MSR, which does not allow radio-frequency (RF) artifacts to pass through the acquisition cable and interfere with the MEG recordings. A fiber-optic system for recording skin conductance – similar to ours – was first proposed by Lagopoulos et al. (2005). However, this system was designed for use in fMRI serving its needs and not in an MEG setup. The main problem somebody faces when attempts to record electrophysiological data inside the MRI room and transmits these data outside, is the powerful alternating magnetic field environment that prohibits placing metallic cables and electrical components in close proximity to the magnetic bore (Lagopoulos et al., 2005). Powerful RFs, which are present in the MRI room, affect severely any conductive cable placed inside the room that acts as a RF antenna. By placing a conductive cable in the MRI scanner room in order to simultaneously record SCR, you (i) introduce artifacts in the MRI scanner, that severely compromise the quality of the acquired images, and (ii) introduce strong artifacts to the recorded SCR signal from the magnetic gradients. The difficulties somebody faces when he/she would like to record SCR signals simultaneously with MEG recordings are different. The presence of a conductive cable inside the MSR that transmits the data in an external computer can bring RFs inside the room canceling the main purpose of the MSR to eliminate RFs radiation, which would degrade SQUID performance. Yet, the presence of any metallic and electrical component in close proximity to the SQUIDs can severely affect the quality of the recorded MEG signal. In both setups, the optical isolation will not allow RF artifacts to pass through the acquisition cable and interfere with the MEG recordings and distort the MRI images respectively. Additionally, the optical fiber in the MRI setup – compared to metallic cabling – is insensitive to the magnetic field of the scanner that may generate severe artifacts in the SCR signal.

The development, calibration, and testing of our system are described and discussed here by using techniques such as skewness and kurtosis, Power Spectral Density (PSD) and the average spectral kurtosis (SK). Once the overall operation reached the required performance level the system was used in an experimental paradigm assessing the emotional processing of healthy human participants.

2. Materials and methods

2.1. Design of the MEG-compatible SCR system

The principal idea for measuring SCRs is to impose a constant DC voltage across two Ag/AgCl electrodes and to measure the changes in the flow of current as a result of the skin conductivity alterations. The MEG-compatible SCR system consists of five integrated circuits (Fig. 1). These were implemented within two separate units: the main recording unit placed inside the MSR and the demodulator unit that is placed outside the MSR. The main recording unit records, amplifies, filters and finally modulates the SCR data to optical signal, while the demodulator unit converts the optical signal to voltage. Both units are powered by batteries. The two units are connected through a fiber optic connection in order to eliminate the transfer of RF from outside the MSR inside distorting the MEG signal with technical artifacts. The fiber-optic cable exits the MSR

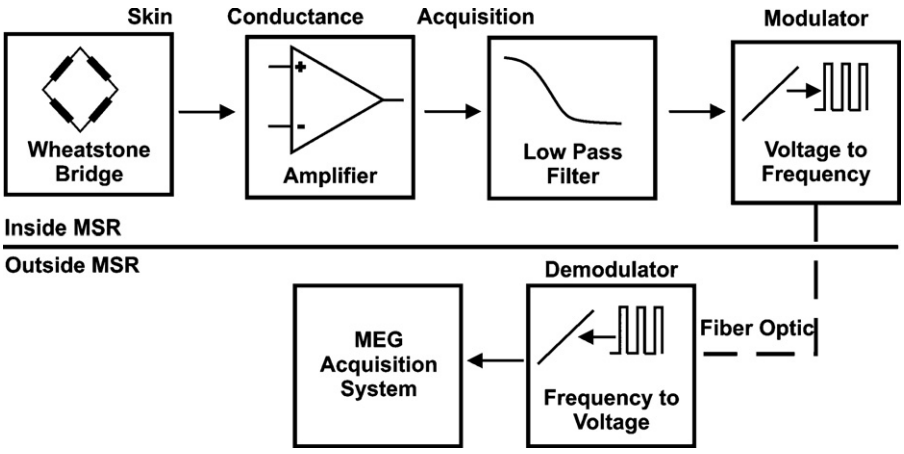

Fig. 1. Block diagram of the MEG-compatible SCR system depicting the flow of the SCR signal.

wall through a penetration panel. The SCR signal is converted into an optical one using the voltage-controlled oscillator (VCO) and is transmitted through the fiber-optic cable outside the MSR where is demodulated and acquired. The VCO is an efficient technique of transmitting information on a series of pulses employed in a wide variety of applications. The data being transmitted are encoded on the frequency of these pulses. The pulses' frequency represents the amplitude of the input's analog signal or wave.

2.2. SCR main recording unit

2.2.1. Development

The design was based on the frequency and amplitude characteristics of SCRs. The values of human SCRs magnitudes range from ~ 0.01 μS to ~1 μS (microSiemens) (Fowles et al., 1981; Dawson et al., 1990). The SCR main recording unit can be distinguished in two sub-units; the SCR sub-unit that consists of a Wheatstone bridge, an amplifier and a filter (Fig. 2) and the modulator sub-unit (Fig. 3). The SCR sub-unit is based on previous work (Shastri et al., 2001) and the background theory is presented in Appendix A. The Wheatstone bridge's design and use is discussed elsewhere (Fowles et al., 1981). In brief, the bridge circuit measures the value of the unknown resistance (R_4) of the human skin. It balances two legs of the bridge circuit with known resistance value (R_1, R_2, R_3) with one leg that includes the unknown resistance.

Two 1N4148 diodes (Discrete Semiconductors: http://www.nxp.com/documents/data_sheet/1N4148_1N4448.pdf) are connected in series in order to produce a forward voltage value of 1.4 V (voltage across each diode is 0.7 V) having a role in stabilizing possible small variations at point A (Fig. 2). Thus, V_{in} at point A is:

$$V_{in} = 1.4 \times \frac{R_7}{R_6 + R_7} = 1.4 \times \frac{0.5k}{0.75k + 0.5k} = 0.56\,\text{V} \quad (1)$$

V_{in} was experimentally measured at 0.562 V. Resistor (R_5) limits current through the two 1N4148 diodes and satisfies that:

$$R_5 \cong \frac{V_+ - 1.4\,\text{V}}{5\,\text{mA}} \quad (2)$$

Following, the output of the Wheatstone bridge is driven to a differential amplifier chip, AD624AD (Analog Devices: http://www.datasheetcatalog.org/datasheet/analogdevices/AD624BD.pdf), designed for a gain of 1000 (Fig. 2). In turn, the differential amplifier feeds a low-pass filter with a 3 dB cutoff frequency of 1 Hz. The two-pole, Butterworth low-pass filter chosen is designed according to UAF42AP requirements on external components, resistors and

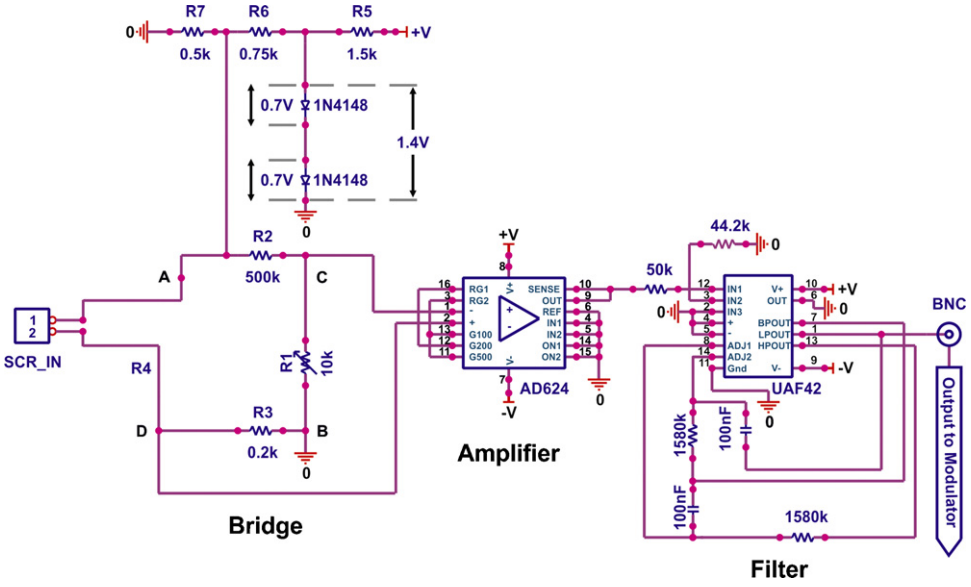

Fig. 2. Schematic design of the SCR sub-unit consisting of a Wheatstone bridge, a differential amplifier (AD624) and low pass filter (UAF42). The filter output is driven to the modulator sub-unit.

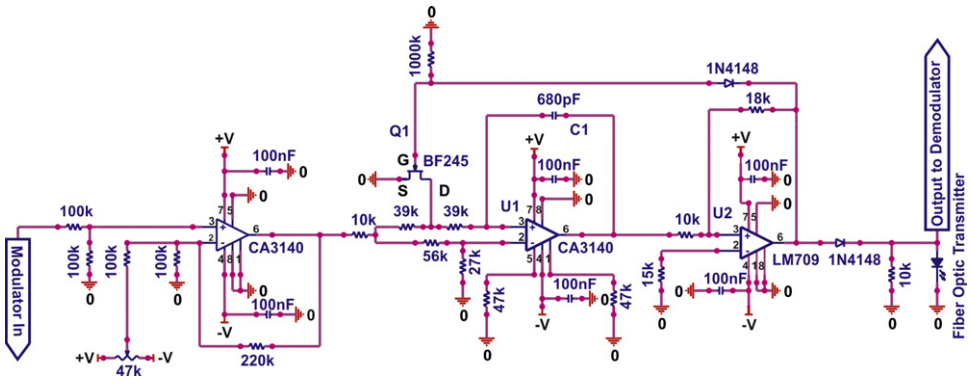

Fig. 3. Schematic design of the modulator sub-unit.

capacitors (Texas Instruments: http://www.ti.com/lit/ds/symlink/uaf42.pdf). Finally, the filter output is driven to the modulator (Fig. 3).

The modulator sub-unit is actually an oscillator whose frequency is determined by a control voltage. The filter output of the SCR sub-unit serves as the control voltage. The core of the modulator sub-unit is the integrator circuit that consists of U1 (CA3140) (Intersil: http://www.intersil.com/data/fn/fn957.pdf) and the capacitor C1 (Fig. 3). The MOSFET Q1 (BF245) (Micro-Electronics: http://pdf1.alldatasheet.com/datasheet-pdf/view/75218/MICRO-ELECTRONICS/BF245.html) is responsible for discharging the capacitor C1 and when combined with the integrator circuit, it produces at the output stage a saw-tooth wave with a frequency proportional to the input voltage level. The final stage U2 (LM709) (National Semiconductor: http://www.ee.nsysu.edu.tw/lab/F6027/LM709%20Operational%20Amplifiers.pdf) serves the pulse wave output by modulating the saw-tooth wave output of the U1 and Q1 network.

Fig. 4 illustrates the SCR main recording unit that houses the circuits previously discussed. SCR signal inputs this unit through a separate electronic plate that consists of two electrodes that are connected to the main unit via a Hi-Flex cable (combination of coaxial and twisted paired cables). There is one on/off switch. Two leds (red and green) on the top of the unit indicate the power condition of the batteries. Moreover, a potentiometer (Fig. 2, R_1) located at the left side is used for the system's calibration. The SCR main recording unit has two outputs: one is a BNC output of the SCR that does not undergo voltage-to-frequency conversion; and the other output is the modulator unit's output that undergoes voltage-to-frequency conversion and serves as input to the demodulator circuit. The two outputs served the testing procedure so as to examine the effect of the modulation and demodulation on the SCR signal.

2.2.2. Calibration

It is considered that the response of the skin and muscle tissue to external and internal stimuli varies the conductance by several μS. Thus, correct calibration is required so as to ensure that the system can measure such subtle differences. The skin has electric properties that change on the relatively short time scale of seconds and are closely related to psychological processes. Specifically, in order to have this variable suppression calibrated, a 10-turn calibrated potentiometer (R_1) is used (Fig. 2). The purpose of the potentiometer is to balance the Wheatstone bridge according to the equation

$$\frac{R_1}{R_2} = \frac{R_4}{R_3} \tag{3}$$

The background theory for the calibration is presented in Appendix B. Estimated values presented in Table B.1, highlight that the system's main recording unit operates at good accuracy for the means of measuring SCRs.

2.3. Demodulator unit

The design of the demodulator (Fig. 5) is based on the LM2917 Frequency to Voltage Converter (National Semiconductor: http://www.jaycar.com.au/images_uploaded/LM2907.PDF). The external components (C_1 = 4.7 nF and R_1 = 68 k) affect the output voltage (V_{out}) according to the input frequency (F_{in}) as follows

$$V_{out} = V_+ \times F_{in} \times C_1 \times R_1 \times K \tag{4}$$

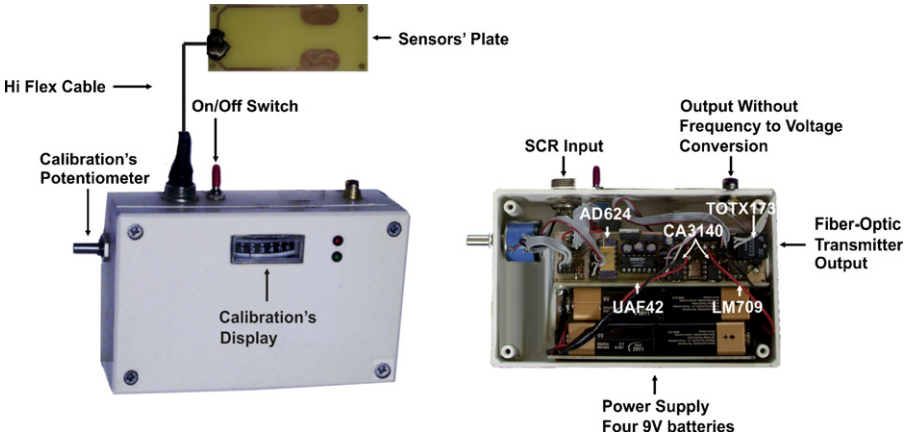

Fig. 4. SCR main recording unit. The external view on the left depicts the actual unit as developed, tested and used for our purposes. On the right, the internal view depicts the components in use.

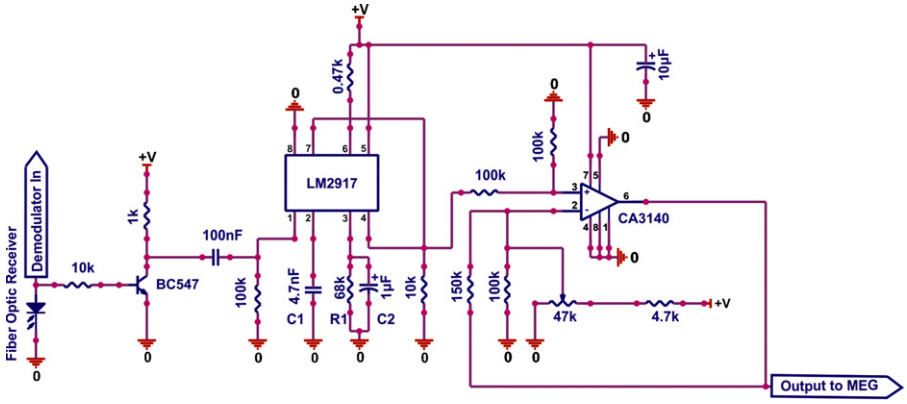

Fig. 5. Schematic design of the demodulator unit.

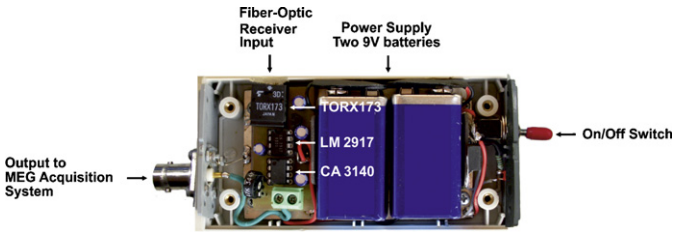

Fig. 6. Demodulator unit. The internal view depicts the components in use.

where V_+ is the power voltage, F_{in} is the frequency of the pulses transmitted by the main recording unit and K is the gain constant which is usually 1.0 according to ICs specifications. The output stage of the demodulator (CA3140) is considered as a buffer stage.

Fig. 6 illustrates the demodulator unit. The unit has one on/off switch and a led on the side of the unit that indicates the power condition of the batteries. The unit has a fiber optic input adaptor for establishing connection to the main recording unit and an output for connecting the unit to the MEG acquisition system. The cable connecting the unit with the acquisition system is a shielded coaxial cable with braided copper sheath.

3. Experimental

3.1. Testing and results

SCR testing took place at the Laboratory for Human Brain Dynamics (1998–2009), Brain Science Institute (BSI), RIKEN, Japan. Magnetic fields were recorded using a 151-channel CTF whole head system (VSM MedTech Ltd., B.C., Canada) inside the MSR. The CTF MEG system is equipped with synthetic 3rd gradient balancing, an active noise cancelation technique that uses a set of reference channels to subtract background interference. For the means of testing our system in the MSR, five male participants were recruited.

MEG measurements were recorded simultaneously to SCRs so as to ensure that the developed MEG-compatible SCR system does not generate unacceptable high levels of noise in these measurements. Two measurements were performed for each participant; one without the unit in the MSR room, and one with the unit in the MSR room. In both measurements, participants were resting with eyes open fixating on a cross. Electrooculographic (EOG) and electrocardiographic (ECG) electrodes were placed on participants. To monitor participants' eye movements, we placed one pair of EOG electrodes 1 cm above and below the left eye (vertical movement) and another pair 1 cm lateral to the left and right outer canthus of the eyes (horizontal movement).

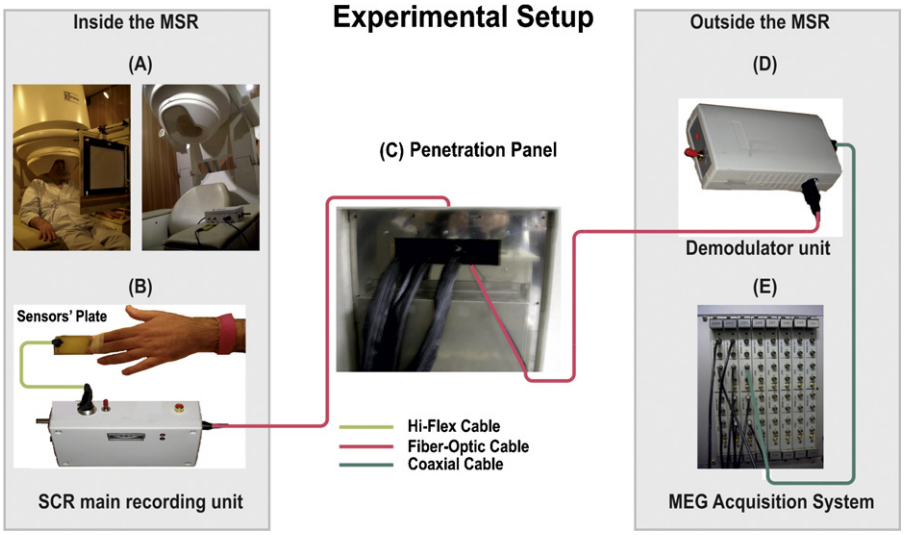

Fig. 7. Configuration for the MEG/SCR system. (A) The participant sits comfortably in an upright position under the helmet-shaped base of the dewar. (B) The index and middle fingers are placed onto the sensors' plate. (C) and (D) The SCR signal travels via the fiber-optic cable and as it is passed through the penetration panel it is fed into the input of the optic transformation device. (E) Finally, the transformed signal is fed into the external channel of the MEG acquisition system which allows the host computer to make the data collection.

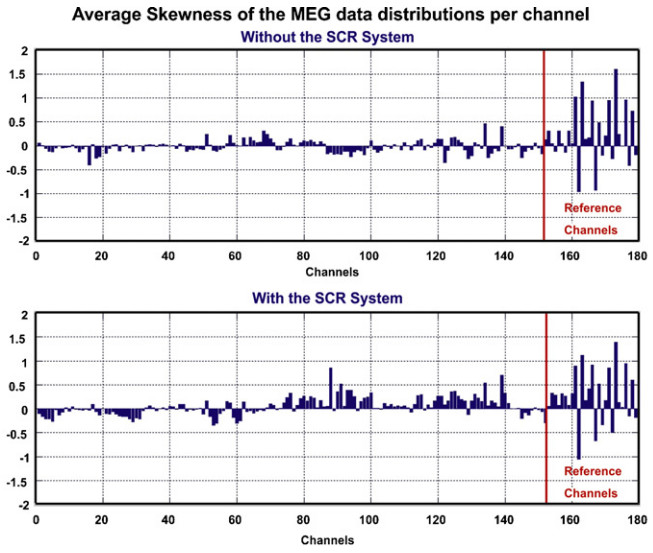

Fig. 8. Average skewness of the MEG signals from all channels (both MEG sensors and reference channels) for both sessions with and without the SCR system.

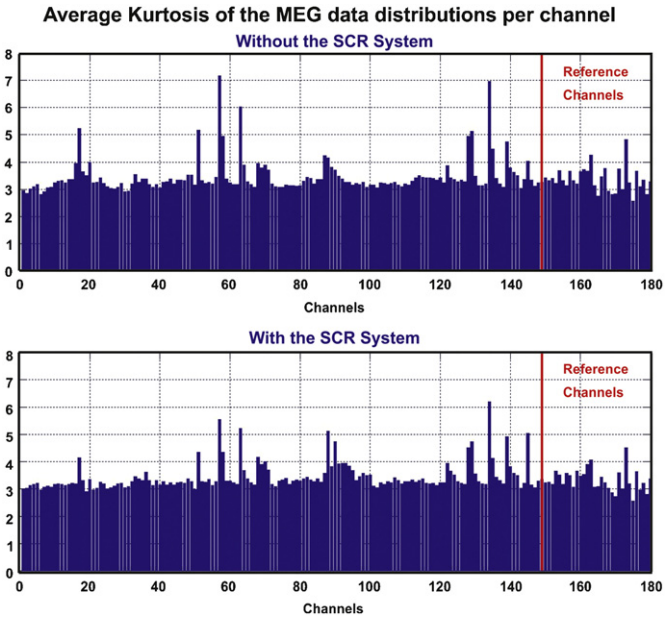

Fig. 9. Average kurtosis of the MEG signals from all channels (both MEG sensors and reference channels) for both sessions with and without the SCR system.

During the second measurement, the fingers' distal sites of the participants were fixed on the sensors' plate and the SCR system was utilized. The distal sites were chosen as the most sensitive body locations for measuring SCR since Scerbo et al. (1992) found that the distal sites provide raw mean skin conductance amplitude two times greater than the medial site. The sensors came into contact with the skin using a conductive paste. Tape was used in order to immobilize the fingers on the sensors' plate while maintaining uniform pressure between the electrodes and the participant's skin, thus reducing the likelihood of spurious signals. Fig. 7 illustrates the MEG/SCR configuration that was set during the experimental procedures described.

The measurements' duration was 120 s with a sampling frequency of 2083 Hz. The MEG data were filtered by a 3rd gradient filter and the DC component was removed from the recordings. The MEG data was post-processed in both time and frequency domain by using Matlab.

The skewness and the kurtosis (see theory/calculation) of the time domain distribution of each signal were estimated for segments of one sec MEG signals. For each recording, the skewness and the kurtosis measures were averaged per channel (for both MEG sensors and MEG reference channels). Figs. 8 and 9 present the averaged skewness and kurtosis results per channel across subjects for the two sessions: with the unit and without the unit. One-way repeated measures of analysis of variance (ANOVA) were performed for the averaged skewness and kurtosis measures with independent variable the presence of the SCR device in the MSR. The ANOVA was performed for all channels and was corrected for multiple comparisons by using Bonferroni corrections. All statistical analyses were performed using SPSS 11.0 J (SPSS, U.S). Differences with values of $p < 0.05$ were considered significant. Data are shown as means ± standard errors unless otherwise stated. No statistical significant differences were observed between the two sessions for neither skewness (see Supplementary Table 1) nor kurtosis (see Supplementary Table 2) for any channel ($p > 0.05$).

Additionally, in the spectral domain we estimated the Power Spectral Density (PSD) since it has been found to be a sensitive measurement to changes of SNR. Assuming that the MEG data of each trial (3 s) satisfy the stationary criterion, the PSD of the MEG sensors and the MEG reference channels was estimated for each trial by using the nonparametric Thompson's Multitaper Method (MTM). Each channel's PSD of each trial was averaged point-by-point and the averaged PSD for each measurement was estimated for both MEG sensors (Fig. 10) and reference channels (Fig. 11). The average PSD for all reference channels of each measurement was also estimated (Fig. 12). Additionally, the average spectral kurtosis (SK) (see theory/calculation) of MEG data was estimated for each channel and each measurement. For both the average PSD and the average SK, ANOVA was performed between the measurements with and without the system. There were no significant statistical differences (see Supplementary Table 3) between the two sessions for neither the MEG sensors nor the MEG reference channels.

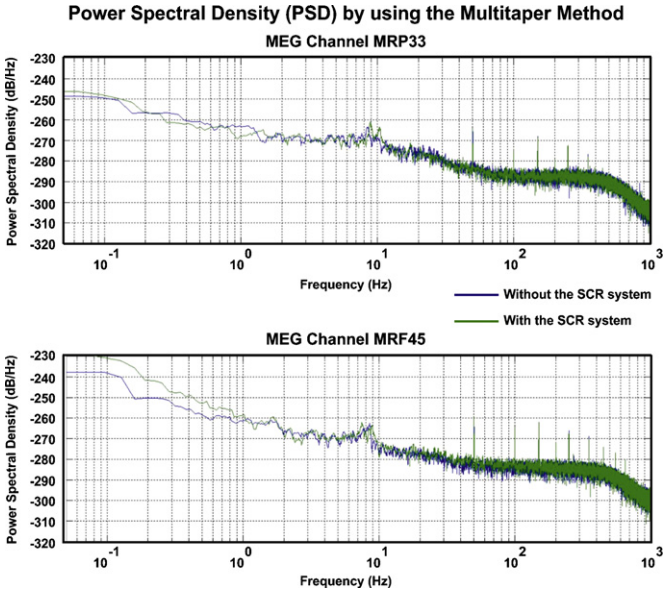

Fig. 10. PSD (in dB/Hz) of MEG signals from MEG channels MRP33 and MRF45 for the measurements of a single participant, with and without the SCR system.

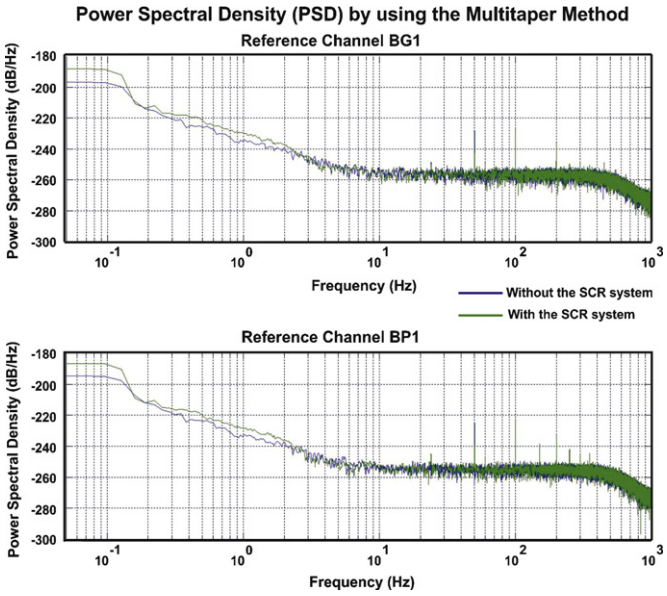

Fig. 11. PSD (in dB/Hz) of MEG signals from reference channels BG1 and BP1 for the measurements of a single participant, with and without the SCR system.

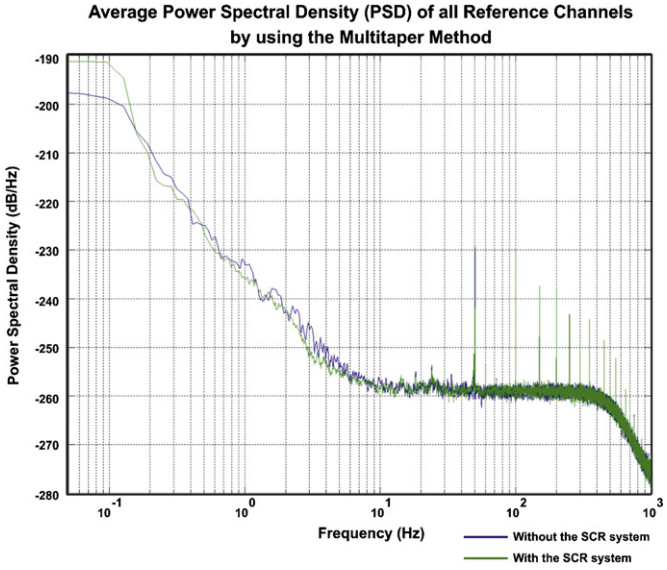

Fig. 12. Average PSD (in dB/Hz) of MEG signals from all the reference channels, for the measurements of a single participant, with and without the SCR system.

4. Theory/calculation

Usually, the characterization of a data set relies on estimates of mean and variance and it can be further characterized by skewness and kurtosis. Skewness is a measure of symmetry, or more precisely, the lack of symmetry. Kurtosis is a measure of whether the data are peaked or flat relative to a normal distribution (Mendel, 1991). Kurtosis provides a measure of distance to Gaussianity (Cohen, 1986). Skewness and kurtosis are used to demonstrate statistical differences in the presence of high noise in a signal (SNR) (Cohen, 1986). Based on these characteristics for the time domain, the effect of the SCR main recording unit interference in the MEG sensors and reference signals was estimated. For univariate data y_1, $y_2, y_3, \ldots, y_n$ the formula of skewness (Brillinger, 1981) is

$$\text{skewness} = \frac{\sum_{i=1}^{N}(y_i - \bar{y})^3}{(N-1)s^3}, \tag{5}$$

where $\bar{y}$ is the mean of the data, s is the standard deviation, and N is the number of samples. For univariate data $y_1, y_2, y_3, \ldots, y_n$ the formula of kurtosis (Brillinger, 1981) is

$$\text{kurtosis} = \frac{\sum_{i=1}^{N}(y_i - \bar{y})^4}{(N-1)s^4}, \tag{6}$$

where $\bar{y}$ is the mean of the data, s is the standard deviation, and N is the number of samples.

A fourth order spectral analysis tool named spectral kurtosis (SK) was also used in order to compare the harmonic content of the MEG signals obtained with and without the system. This tool provides additional information with respect to classical second order spectral quantities (Dwyer, 1984). In the frequency domain, the spectral kurtosis (SK) of a signal is defined as the kurtosis of its frequency components. It is a powerful tool of detecting "randomly occurring" signals (Vrabie et al., 2003). In the case of finite length random process, the spectral kurtosis (SK) can be defined as

$$SK_x^N(m) = \frac{Cum[X_n(m), X_N(m), X_N^*(m)X_N^*(m)]}{(Cum[X_N(m), X_N^*(m)])^2} \tag{7}$$

where $X_N(m)$ is a complex random variable given by the N-points Discrete Fourier Transform (DFT) of $X_N(n)$

The global field power (GFP) was estimated for each experimental condition and each participant allowing estimation of the major components. GFP is a global and well-established quantifier of scalp field strength (Lehmann and Skrandies, 1980, 1984). It is estimated as the square root of the sum of squares of the magnetic measurements over the sensors for each data point in the filtered and averaged epoch:

$$\text{GFP} = \frac{1}{N} * \sqrt{(s_{x^2})} \tag{8}$$

where N is the number of sensors which measure the fields and S_x is the mean magnetic field of all sensors.

5. Affective experiment

Simultaneous MEG/SCR recordings took place at the Laboratory for Human Brain Dynamics (1998–2009), Brain Science Institute (BSI), RIKEN, Japan using the same materials as those for its testing (see Section 3.1).

Our SCR system was tested within an affective experiment of twelve healthy participants with normal or corrected to normal visual acuity (7 males, mean age 30.8 ± 5.3, range 23–40 years, 5 females mean age 27.8 ± 5.3, range 21–35 years). The study was approved by the host's ethics committee and all participants gave written informed consent prior to participation. The methods and results of this study will be published elsewhere.

Participants passively viewed pictures from the International Affective Picture System (IAPS) collection (Lang et al., 1993) categorized within four sets (pleasant and high arousing (PHA), pleasant and low arousing (PLA), unpleasant and high arousing (UHA) and unpleasant and low arousing (ULA)) that manipulated the level of arousal within pleasant and unpleasant pictures (Cuthbert et al., 1996). The stimuli were presented centered on the screen in a mixed fashion for 1 s after the appearance of a fixation cross centered on the screen for a pseudo-randomized interval of 1.5 ± 0.2 s.

MEG recordings were filtered by a 3rd gradient filter and the DC component was removed from the measurements. Also, these were filtered by high-pass filtering at 2 Hz, low-pass filtering at 30 Hz, power-line notch filtering at 50 Hz and its harmonics. Following was segmentation into epochs, each one lasting 1 s after the onset of the stimuli according to the four conditions' events (PHA, PLA, UHA, ULA), removal of the baseline for −0.3 to 0 s and averaging in respect to the stimulus onset from −0.3 to 1 s.

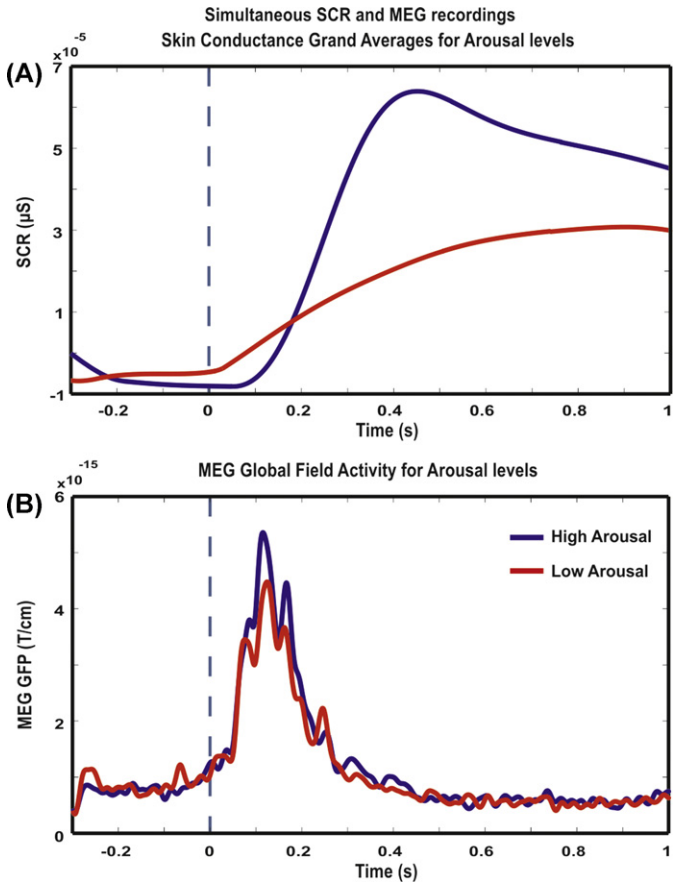

Fig. 13. Simultaneous SCR and MEG recordings. (A) Grand average of SCRs for high and low arousal. Stimulus onset was at 0 s. (B) Averaged MEG GFP activity for high and low arousal. Stimulus onset was at 0 s.

Source activity was estimated by using a beamforming technique, the Synthetic Aperture Magnetometry (SAM) (Robinson and Vrba, 1998; Singh et al., 2002, 2003; Cheyne et al., 2006; Hillebrand et al., 2005) at the target frequency. SAM images were used to generate a group SAM image (Singh et al., 2002, 2003).

SCR recordings were filtered using low-pass filter with cut-off frequency at 2.5 Hz. Following was segmentation into epochs, removal of the baseline for −0.3 to 0 s and averaging in respect to the stimulus onset from −0.3 to 1 s. The grand average was also calculated across all participants.

After the closure of the BSI MEG laboratory the data were anonymized and transferred to the Laboratory for Human Brain Dynamics, at AAI Scientific Cultural Services Ltd., in Nicosia, Cyprus for follow up research and data analysis.

6. Results

Fig. 13 depicts the grand average of the SCRs for high and low arousal for 2.5 Hz (Fig. 13A) as well as the GFP of grand-averaged ERFs for a wideband of 2–30 Hz (Fig. 13B). Fig. 14 presents the localization results of the main arousal effect for a wideband of 2–30 Hz across participants. Significant differences ($p < 0.001$, uncorrected) between high and low arousing images were observed on right inferior parietal lobule (IPF) (Fig. 14, left-middle side) at MNI coordinates x: 46, y: −30, z: 30; cluster size: 358 voxels; t-values for each peak: 3.37. Also differences in arousing images were localized on the right temporal pole (TP) (Fig. 14, middle-right side) at MNI coordinates x: 54, y: 8, z: −14; cluster size: 327 voxels; t-values for each peak: 3.37.

7. Discussion

Our work addressed important economic and compatibility issues by introducing a low-cost MEG-compatible SCR system that allows simultaneous recordings of SCR and MEG which assess the autonomic and the central nervous system activity respectively. The challenge in these simultaneous recordings is to obtain artifact free MEG recordings, while introducing into the MSR electrical equipment for the recording of SCR. In order to produce a system compatible to the MEG environment, we followed previous suggestions (Shastri et al., 2001; Lagopoulos et al., 2005) and extended them based on the biomagnetism principles. The special feature of our system is the optical isolation between the two units one placed inside and the other outside the MSR, which does not allow RF artifacts to pass through the acquisition cable and interfere with the MEG recordings.

The system was designed for continuous monitoring of SCR and specifically for neuroscience experiments that focus on emotional processing as the one reported here. To the best of our knowledge, such a system is not available in the MEG community and this may explain the fact that the literature reporting such kind of measurements is limited to a single study. There are alternative but expensive solutions and some may indeed be available in other MEG laboratories. MEG-compatible commercial EEG systems that include an SCR recording module are expensive (>$70,000). The design of our system is simple allowing its implementation by neuroscientists who do not have specialized knowledge in electronics, and its implementation costs <$200.

The results of testing our system demonstrate no significant differences in any of the statistical indices we computed between the

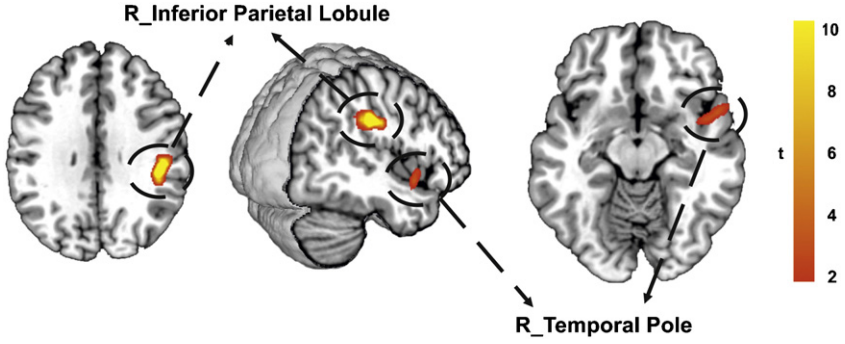

Fig. 14. Group SAM image for arousal main effect. Arousal correlated to decreases on right inferior parietal lobule and right temporal lobe. Points counted as left or right were at least 6 mm from the midline. The brain region is superimposed with orthogonal sections (sagittal, coronal, and axial) of an anatomical scan rendered in standard Montreal Neurological Institute (MNI) space. The corresponding t-values are shown in the color scale for all contrasts. Uncorrected $p < 0.001$ was adopted as the height threshold; minimum is ten contiguous voxels.

two sessions (without the unit in the MSR; and with the unit in the MSR, connected to the participant, and in operation). Thus, they demonstrate that the developed system does not distort the MEG recordings and can be further used in neuroscience experiments such as the one presented here that focus on emotional processing.

To the best of our knowledge our work represents the first MEG-compatible low-cost SCR system for monitoring SCR in the MSR. The system was tested in an MEG environment and was found to be reliable in the simultaneous recordings of MEG and SCRs. The system applicability was tested in an emotional study.

Acknowledgements

Data acquisition of the modalities described as well as the original analysis of the MEG signals was conducted at the Laboratory for Human Brain Dynamics (1998–2009), Brain Science Institute (BSI), RIKEN, Japan by CP. The work continued and was finalized at the Aristotle University of Thessaloniki and the Laboratory for Human Brain Dynamics, AAI Scientific Cultural Services Ltd. with partial support from the Cyprus Research Promotion Foundation grant ΑΝΑΒΑΘΜΙΣΗ/ΠΛΗΡΟΣ/0308/02 and ΕΠΙΧΕΙΡΗΣΕΙΣ/ΠΡΟΙΟΝ/0609/76, and co-funded by the European Regional Development Fund of the E.U.

Appendix A.

Methods referring to the SCR unit have been already published (Shastri et al., 2001). The voltage output of the bridge across points C and D (Fig. 2) is given by:

$$V_{out} = V_{in} \cdot \left(\frac{R_1}{R_1 + R_2} - \frac{R_3}{R_3 + R_4} \right) \quad (A.1)$$

where V_{in} is the voltage difference between points A and B (ground) and R_1, R_2, R_3, are the known resistors of the bridge (10 kΩ variable, 500 kΩ, and 200 Ω, respectively). R_4 is the unknown resistance of the participant's skin. Given the resistance values and noting that the skin resistances are on the order of 10^5 Ω or greater, then:

$$R_1 \ll R_2$$

$$R_3 \ll R_4$$

Thus Eq. (A.1) is simplified as follows:

$$V_{out} = V_{in} \cdot \left(\frac{C_2}{C_1} - \frac{C_4}{C_3} \right) \quad (A.2)$$

where the conductance $C_n = 1/R_n$ with $n = 1, 2, 3, 4$.

The bridge is balanced by adjusting C_1 until V_{out} is zero. Change in the bridge output voltage due to subsequent changes in the participant's skin conductance C_4 is given by:

$$\Delta V_{out} = -V_{in} \cdot \left(\frac{\Delta C_4}{C_3} \right) \quad (A.3)$$

After amplification, the total output voltage ΔV_{total} is

$$\Delta V_{total} = -GV_{in} \cdot \left(\frac{\Delta C_4}{C_3} \right) \quad (A.4)$$

Eq. (A.4) can also be written as follows:

$$\Delta C_4 = -\Delta V_{total} \beta \quad (A.5)$$

where

$$\beta = \frac{C_3}{GV_{in}} \quad (A.6)$$

Table B.1
Values of the external resistors connected to SCR sensors and the corresponding output voltages. For each pair of measurements, β was estimated and found to be in good agreement with the theoretically expected value.

R (KΩ)	V_{out} (mV)	Experimentally measured β	Theoretically expected β	Error
1514	56.9			
388	271	8.9529		0.631%
220	492	8.9056		0.099%
184	590	9.0748	8.8968	2.000%
147.5	738	9.0870		2.138%
119.8	914	8.9067		0.112%
100	1096	9.0811		2.071%

Appendix B.

Methods referring to the calibration of the SCR unit have been already published (Shastri et al., 2001). The participant's skin conductance amplitudes,

$$\Delta C_4 = \frac{1}{R_4} \quad (B.1)$$

are related to the amplified output voltage of the skin conductance circuit by

$$\Delta C_4 = -\Delta V_{total} \times \beta \quad (B.3)$$

where $\beta = C_3/(GV_{in})$

For our skin conductance circuit it is given:

$$C_3 = \frac{1}{R_3} = \frac{1}{0.2k} = 5 \times 10^{-3} \text{ mS}, V_{in} = 0.562 \text{ V}, G = 1000 \quad (B.4)$$

Thus, it is expected that theoretically $\beta = 8.8968$ μS/V. Moreover, since C_3, V_{in}, and G are known to within 1%, it can be shown that β should have an uncertainty of 3%. In order to check the system's accuracy, external accurate resistors were connected in series across the SCR sensors and V_{out} was measured. In addition, β was experimentally estimated by sampling V_{out} while the external resistors were connected to the SCR sensors (Table B.1). The calibration procedure indicated that all measured β values were in the range of 3%. Thus, the SCR main recording unit operates at good accuracy for the means of measuring SCRs.

Appendix C. Supplementary data

Supplementary data associated with this article can be found, in the online version, at http://dx.doi.org/10.1016/j.jneumeth.2012.09.026.

References

Bamidis PD, Papadelis C, Kourtidou-Papadeli C, Pappas C, Vivas A. Affective computing in the era of contemporary neurophysiology and health informatics. Interact Comput 2004;16(4):715–21.
Bernat E, Patrick CJ, Benning SD, Tellegen A. Effects of picture content and intensity on affective physiological response. Psychophysiology 2006;43:93–103.
Boucsein W. Electrodermal activity. Springer: Berlin; 1992.
Brillinger DR. Time series, data analysis and theory. Expanded ed. San Francisco: Holden-Day Inc.; 1981.
Cheyne D, Bakhtazad L, Gaetz W. Spatiotemporal mapping of cortical activity accompanying voluntary movements using an event-related beamforming approach. Hum Brain Mapp 2006;27(3):213–29.
Cohen A. Biomedical signal analysis. Time and frequency domain analysis, vol. I. Florida: CRC Press; 1986.
Critchley HD, Elliott R, Mathias CJ, Dolan RJ. Neural activity relating to generation and representation of galvanic skin conductance responses: a functional magnetic resonance imaging study. J Neurosci 2000;20:3033–40.
Cuthbert BNN, Bradley MM, Lang PJ. Probing picture perception: activation and emotion. Psychophysiology 1996;33:103–11.
Dawson ME, Schell AM, Filion DL. The electrodermal system. In: Cacioppo JT, Tassinary LG, editors. Principles of psychophysiology. Cambridge: Cambridge University Press; 1990. p. 295–325.

Dwyer RF. Use of the kurtosis statistic in the frequency domain as an aid in detecting random signals. IEEE J Oceanic Eng OE 1984;9(2):85–92.
Fowles DC, Christie MJ, Edelberg R. Publication recommendations for electrodermal measurements. Psychophysiology 1981;18:232–9.
Hamalainen MS, Hari R, Ilmoniemi RJ, Knuutila J, Lounasmaa OV. Magnetoencephalography – theory, instrumentation, and applications to noninvasive studies of the working human brain. Rev Mod Phys 1993;65:413–98.
Hillebrand A, Singh KD, Holliday IE, Furlong PL, Barnes GR. A new approach to neuroimaging with magnetoencephalography. Hum Brain Mapp 2005;25: 199–211.
Ioannides AA, Sargsyan A. Rhythmogram-based analysis for continuous electrographic data of the human brain. IEEE Trans Inform Technol Biomed 2012;16:205–11.
Lagopoulos J, Malhi G, Shnier R. A fiber-optic system for recording skin conductance in the MRI scanner. Behav Res Methods 2005;37(4):657–64.
Lang PJ, Greenwald MK, Bradley MM, Hamm AO. Looking at pictures: affective, facial, visceral and behavioral reactions. Psychophysiology 1993;30:261–73.
Lehmann D, Skrandies W. Reference-free identification of components of checkerboard-evoked multichannel potential fields. Electroencephalogr Clin Neurophysiol 1980;48(6):609–21.
Lehmann D, Skrandies W. Spatial analysis of evoked potentials in man – a review. Prog Neurobiol 1984;23(3):227–50.
Lim CL, Seto-Poon M, Clouston PD, Morris JG. Sudomotor nerve conduction velocity and central processing time of the skin conductance response. Clin Neurophysiol 2003;114:2172–80.
Lithari C, Frantzidis CA, Papadelis C, Vivas AB, Klados MA, Kourtidou-Papadeli C, Pappas C, Ioannides AA, Bamidis PD. Are females more responsive to emotional stimuli? A Neurophysiological study across arousal and valence dimensions. Brain Topogr 2010;23:27–40.
MacIntosh J, Mraz R, McIlroy WE, Graham SJ. Brain activity during a motor learning task: an fMRI and skin conductance study. Hum Brain Mapp 2007;28: 1359–67.
Mendel TM. Tutorial on higher-order statistics (spectra) in signal processing and system theory: theoretical results and some applications. Proc IEEE 1991;79:277–305.
Moradi F, Liu LC, Cheng K, Waggoner RA, Tanaka K, Ioannides AA. Consistent and precise localization of brain activity in human primary visual cortex by MEG and fMRI. Neuroimage 2003;18:595–609.
Ohira H, Nomura M, Ichikawa N, Isowa T, Iidaka T, Sato A, et al. Association of neural and physiological responses during voluntary emotion suppression. Neuroimage 2006;29:721–33.
Papadelis C, Eickhoff SB, Zilles K, Ioannides AA. BA3b and BA1 activate in a serial fashion after median nerve stimulation: direct evidence from combining source analysis of evoked fields and cytoarchitectonic probabilistic maps. Neuroimage 2011;54:60–73.
Papadelis C, Poghosyan V, Fenwick CPBC, Ioannides AA. MEG's ability to localise accurately weak transient neural sources. Clin Neurophysiol 2009;120(11):1958–70.
Robinson SE, Vrba J. Functional neuroimaging by synthetic aperture magnetometry (SAM). In: Yoshimoto T, Kotani M, Kuriki S, Karibe H, Nakasato N, editors. Recent advances in biomagnetism. Sendai: Tohuku University Press; 1998. p. 302–5.
Scerbo AS, Freedman LW, Raine A, Dawson ME, Venables PH. A major effect of recording site measurement of electrodermal activity. Psychophysiology 1992;29:241–6.
Seth AK, Iversen JR, Edelman GM. Single trial discrimination of truthful from deceptive responses during a game of financial risk using alpha-band MEG signals. Neuroimage 2006;32(1):465–76.
Shastri A, Lomarev MP, Nelson SJ, George MS, Holzwarth MR, Bohning DE. A low-cost system for monitoring skin conductance during functional MRI. J Magn Reson Imaging 2001;193(14):187.
Singh KD, Barnes GR, Hillebrand A, Forde EM, Williams AL. Task-related changes in cortical synchronization are spatially coincident with the hemodynamic response. Neuroimage 2002;16:103–14.
Singh KD, Barnes GR, Hillebrand A. Group imaging of task-related changes in cortical synchronisation using non-parametric permutation testing. Neuroimage 2003;19:1589–601.
Vrabie V, Granjon P, Serviere C. Spectral kurtosis: from definition to application. In: Workshop on nonlinear signal and image processing; 2003, NSIP03.
Yamamoto T, Williamson SJ, Kaufman L, Nicholson C, Llinas R. Magnetic localisation of neuronal activity in the human brain. Proc Natl Acad Sci U S A 1988;85:8732–6.